Fermi National Accelerator Laboratory

FERMILAB-Pub-78/36-EXP
7180.178

(Submitted to Phys. Rev. Lett.)

# PROJECTILE DEPENDENCE OF MULTIPARTICLE PRODUCTION IN HADRON-NUCLEUS INTERACTIONS AT 100 GeV/c

J. E. Elias
Fermi National Accelerator Laboratory, Batavia, Illinois 60510

and

W. Busza, C. Halliwell, D. Luckey, L. Votta, and C. Young
Physics Department and Laboratory for Nuclear Science
Massachusetts Institute of Technology, Cambridge, Massachusetts 02139

April 1978

# Projectile Dependence of Multiparticle Production in Hadron-Nucleus Interactions at 100 GeV/c*

J.E. ELIAS

Fermi National Accelerator Laboratory

Batavia, Illinois 60510

and

W. BUSZA, C. HALLIWELL, D. LUCKEY, L. VOTTA, and C. YOUNG

Physics Department and Laboratory for Nuclear Science

Massachusetts Institute of Technology

Cambridge, Massachusetts 02139

Average multiplicities and pseudorapidity distributions for 100 GeV/c p, $K^+$, and $\pi^+$-nucleus collisions are presented. The average multiplicities increase with nuclear thickness. The fractional increase is independent of incident particle species provided that nuclear thicknesses are calculated in units of mean free path of the incident hadron. This scaling behavior suggests that the immediate product of a hadron-nucleon collision is a state similar to the incident hadron.

We have measured the average multiplicities, $\langle n \rangle_A$, and the pseudorapidity distributions of charged, relativistic ($\beta \gtrsim 0.85$) secondaries produced in collisions between an incident hadron (p, $\bar{p}$, $K^+$, $\pi^+$, and $\pi^-$) and a target nucleus (atomic number A) at 50, 100, and 200 GeV/c. This experiment was carried out in the M6 secondary beam at Fermilab, and a brief description of the experiment and the proton-nucleus results were presented in a previous publication.[1] In this Letter, we compare the p, $K^+$, and $\pi^+$ data at 100 GeV/c.

The average multiplicity results, $\langle n \rangle_A$, are given in Table I. A measure of the amount of intra-nuclear multiplication is given by the ratio $R_A = \langle n \rangle_A / \langle n \rangle_H$, where $\langle n \rangle_H$ is the average hydrogen multiplicity. Existing high-energy data[2] indicate that $R_A$ is independent of the incident particle type when the nuclear thickness is measured in terms of $\bar{\nu}$. The parameter $\bar{\nu}$ is the average number of inelastic collisions that the incident hadron h would undergo in traversing the nucleus assuming that all collisions are governed by the cross section of the incident hadron. It should be noted that for all collisions other than the first, the incident hadron h need not be involved, provided that it is replaced by a state with the same cross section. The values of $\bar{\nu}$ shown in Table I are given by the formula $A\sigma_{hp}/\sigma_{hA}$, where $\sigma_{hp}(\sigma_{hA})$ is the absorption cross section of h on hydrogen (nucleus).[3] Thus $\bar{\nu}$ depends not only on the target nucleus A but also on the incident hadron h.

In contrast to earlier comparisons[4], the data reported here permit a test of this apparent scaling of $R_A$ with $\bar{\nu}$ free from the systematic difficulties involved in combining the data from several experiments. Furthermore, previous to this experiment, no $K^+$-nucleus multiplicity data were available.

Since our hydrogen multiplicities are obtained by a $CH_2$-C subtraction, the uncertainties are relatively large. We have, therefore, chosen to use the multiplicities measured in a bubble chamber experiment[5] in our determination of $R_A$. These multiplicities, $\langle n \rangle_{ch}$, are also given in Table I. Unlike the nuclear multiplicities measured in this experiment, $\langle n \rangle_{ch}$ includes nonrelativistic prongs. We calculate $\langle n \rangle_H$ using the formula $\langle n \rangle_H = \langle n \rangle_{ch} - 0.5$.[6]

Figure 1(a) is a plot of $R_A$ versus $\bar{\nu}$. There is little or no incident particle dependence. The results can be fitted by $R_A = 0.47 + 0.61\bar{\nu}$ with a chi-square of 13 for 10 degrees of freedom. For comparison, Figure 1(b) shows that $R_A$ does not scale with the physical thickness of the target as measured by $A^{1/3}$.

Our data are also inconsistent with the hypothesis that all collisions other than the first are governed by the cross section of a pion rather than that of the incident hadron. We plot $R_A$ against $\bar{\nu}'$ in Figure 1(c). The parameter $\bar{\nu}'$ is the average number of inelastic collisions that the incident hadron h would undergo in traversing the nucleus, assuming that while the initial collision is governed by the cross section

of the incident hadron, all subsequent collisions are governed by the pion cross section. The values of $\bar{\nu}'$ are given by the formula $\bar{\nu}' = 1 + (\bar{\nu} - 1)\sigma_{\pi p}/\sigma_{hp}$.

The scaling of $R_A$ with $\bar{\nu}$ is compatible with a picture in which a beam-like state interacts successively with different nucleons within the nucleus. To investigate further this phenomenon, we examine the multiplicity ratio $r(\eta)$ for different regions of pseudorapidity $\eta = -\ln(\tan(\theta/2))$. As in the determination of $R_A$, the hydrogen values are derived from bubble chamber measurements.[7] Figure 2 shows $r(\eta)$ as a function of $\eta$ interpolated to $\bar{\nu} = 3$. The scaling effect is seen to hold for individual regions of pseudorapidity.

In summary, our data are consistent with models in which the multiplicity increase is governed by the parameter $\bar{\nu}$, independent of the incident particle species. The parameter $\bar{\nu}$ was derived using the assumption that after each collision in the nucleus, the produced state has a cross section equal to that of the incident particle. Therefore we conclude that the immediate product of a hadron-nucleon collision is a state similar to the incident hadron.

FOOTNOTES AND REFERENCES

*Work supported in part by the United States ERDA under Contract No. EY-76-C-02-3069.

1. C. Halliwell et al., Phys. Rev. Lett. 39, 1499 (1977).
2. For example, $\pi^-$-nucleus data from W. Busza et al., Phys. Rev. Lett. 34, 836 (1975); p-W and p-Cr data from J.R. Florian et al., Phys. Rev. D13, 558 (1976); and p-Emulsion data from a compilation by I. Otterlund, Acta Phys. Polon. B8, 119 (1977).
3. The hadron-nucleus cross sections used to calculate $\bar{\nu}$ are from S.P. Denisov et al., Nucl. Phys. B61, 62 (1973). These cross sections were extrapolated to 100 GeV/c using the energy dependence of the hadron-nucleon inelastic cross sections quoted by D.S. Ayres et al., Phys. Rev. D15, 3105 (1977). A Wood-Saxon distribution of nuclear matter was assumed.
4. W. Busza, op. cit., Reference 2.
5. W.M. Morse et al., Phys. Rev. D15, 66 (1977).
6. G. Calucci, R. Jengo, and A. Pignotti, Phys. Rev. D10, 1468 (1974).
7. The rapidity distributions measured in Reference 5 were normalized to $\langle n \rangle_H = \langle n \rangle_{ch} - 0.5$, and were then used to calculate $r(\eta)$. The difference between rapidity and pseudorapidity is ignored. This procedure may distort the shape of $r(\eta)$, but should not affect the comparison of p, $K^+$, and $\pi^+$ results.

TABLE I: The average multiplicities of relativistic charged particles produced in 100 GeV/c hadron-nucleus collisions for several values of $\bar{\nu}$. The errors include all statistical and systematic uncertainties. The bubble chamber multiplicities $\langle n \rangle_{ch}$ of Reference 5 are also shown.

| Target | Projectile | $\bar{\nu}$ | Average Multiplicity |
|---|---|---|---|
| C | $\pi^+$ | 1.27 ± 0.02 | 7.86 ± 0.15 |
| | $K^+$ | 1.24 ± 0.02 | 6.92 ± 0.33 |
| | p | 1.43 ± 0.01 | 7.72 ± 0.16 |
| Cu | $\pi^+$ | 2.01 ± 0.04 | 10.29 ± 0.26 |
| | $K^+$ | 1.85 ± 0.04 | 8.89 ± 1.10 |
| | p | 2.41 ± 0.02 | 11.00 ± 0.32 |
| Pb | $\pi^+$ | 2.77 ± 0.09 | 13.21 ± 0.30 |
| | $K^+$ | 2.47 ± 0.09 | 12.92 ± 0.79 |
| | p | 3.49 ± 0.05 | 14.75 ± 0.38 |
| U | $\pi^+$ | 2.87 ± 0.09 | 14.57 ± 0.39 |
| | $K^+$ | 2.55 ± 0.10 | 12.93 ± 1.33 |
| | p | 3.64 ± 0.05 | 15.94 ± 0.50 |
| Hydrogen Bubble Chamber | $\pi^+$ | 1.0 | 6.62 ± 0.07 |
| | $K^+$ | 1.0 | 6.65 ± 0.31 |
| | p | 1.0 | 6.37 ± 0.06 |

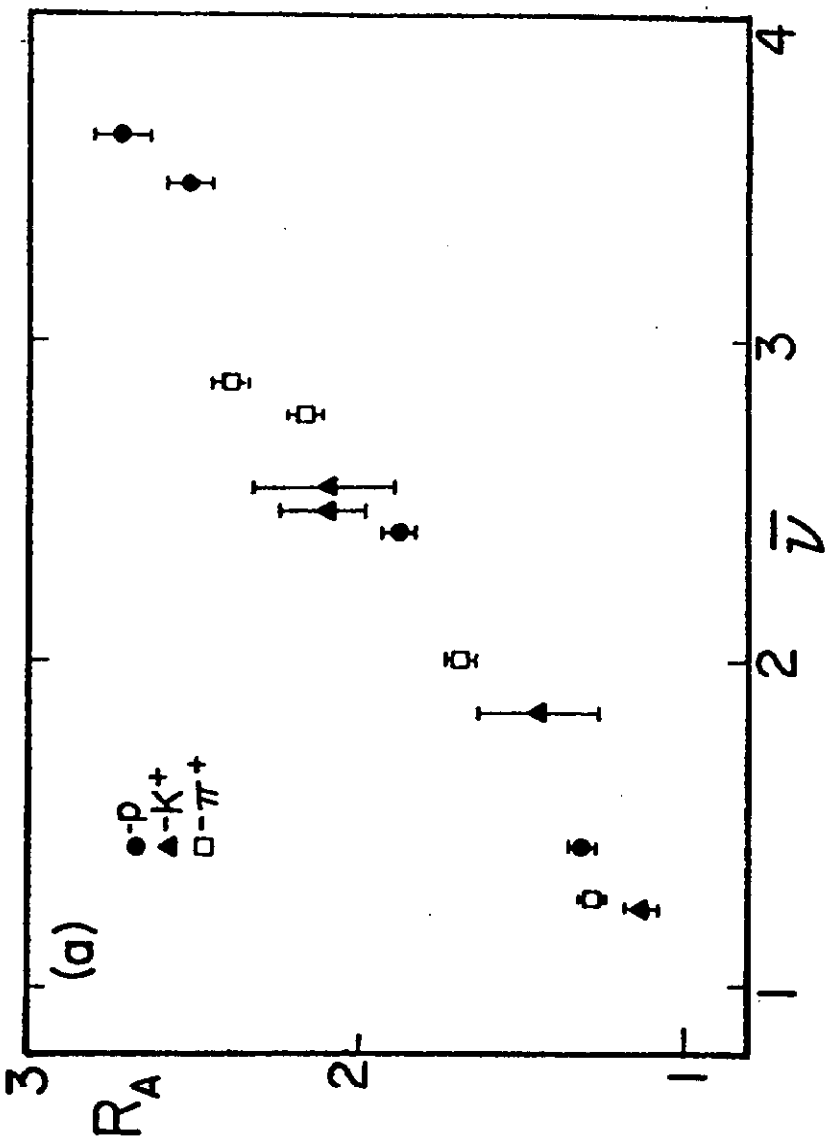


Fig. 1(a). $R_A$ versus $\bar{\nu}$. The errors on the data points include all statistical and systematic uncertainties.

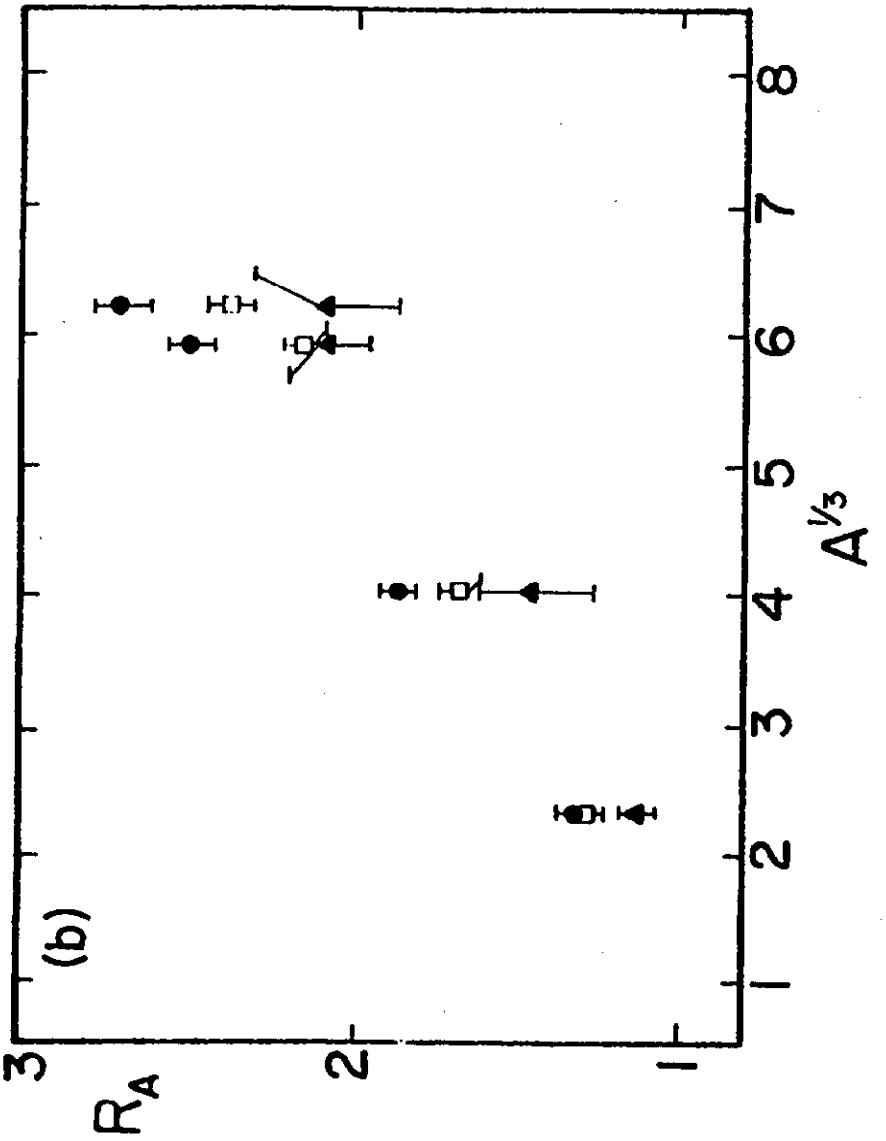


Fig. 1(b). $R_A$ versus $A^{1/3}$. The errors on the data points include all statistical and systematic uncertainties.

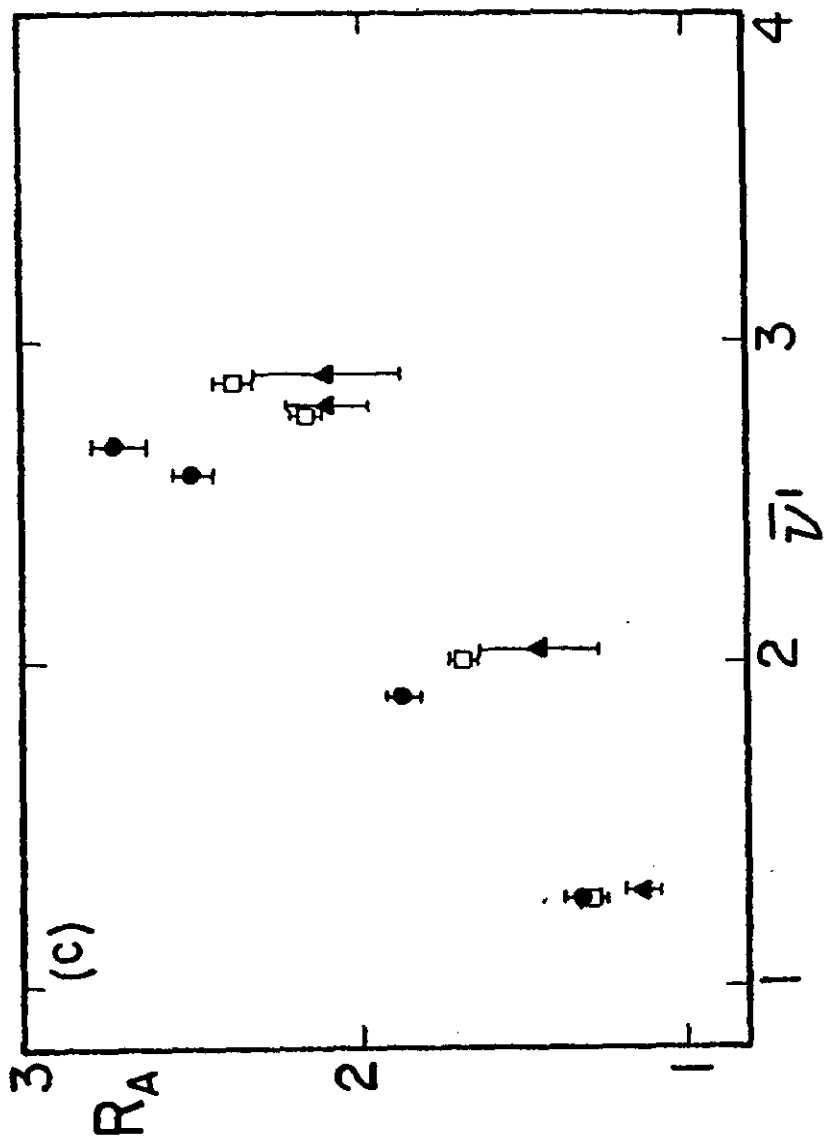


Fig. 1(c). $R_A$ versus $\bar{\nu}$. The errors on the data points include all statistical and systematic uncertainties.

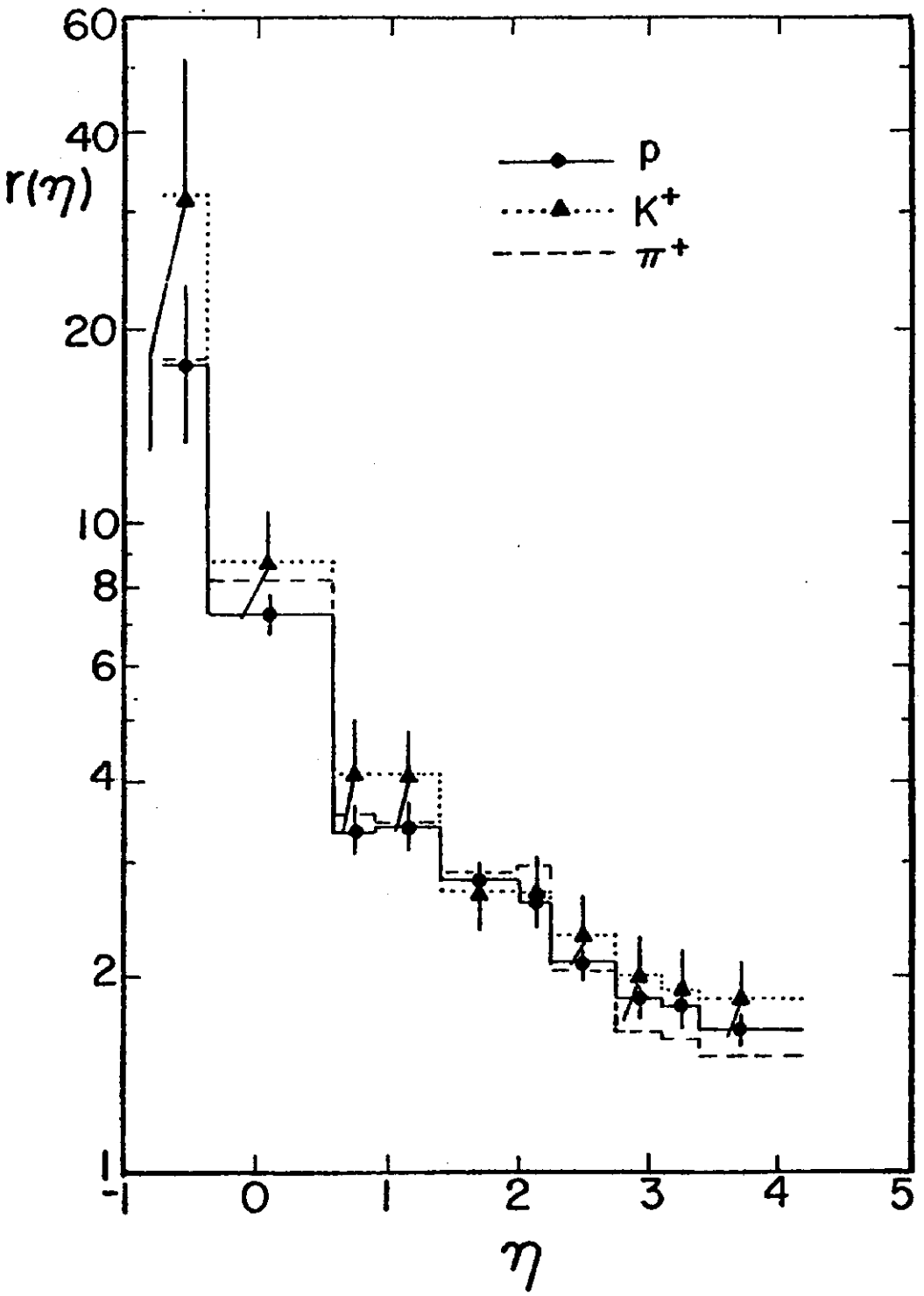


Fig. 2. The multiplicity ratio $r(\eta)$. The errors shown include allsta statistical and systematic uncertainties. In the interest of clarity, errors on the $\pi^+$-induced data are not shown. They are comparable to the proton data. The region $\eta > 4.2$ is not shown because our data in this region have significant systematic uncertainties introduced by acceptance corrections as discussed in Ref. 1.